

A machine learns to predict the stability of circumbinary planets

Christopher Lam^{1*} and David Kipping¹

¹*Dept. of Astronomy, Columbia University, 550 W 120th Street, New York NY 10027*

Accepted . Received ; in original form

ABSTRACT

Long-period circumbinary planets appear to be as common as those orbiting single stars and have been found to frequently have orbital radii just beyond the critical distance for dynamical stability. Assessing the stability is typically done either through N-body simulations or using the classic Holman-Wiegert stability criterion: a second-order polynomial calibrated to broadly match numerical simulations. However, the polynomial is unable to capture islands of instability introduced by mean motion resonances, causing the accuracy of the criterion to approach that of a random coin-toss when close to the boundary. We show how a deep neural network (DNN) trained on N-body simulations generated with REBOUND is able to significantly improve stability predictions for circumbinary planets on initially coplanar, circular orbits. Specifically, we find that the accuracy of our DNN never drops below 86%, even when tightly surrounding the boundary of instability, and is fast enough to be practical for on-the-fly calls during likelihood evaluations typical of modern Bayesian inference. Our binary classifier DNN is made publicly available at <https://github.com/CoolWorlds/orbital-stability>.

Key words: circumbinary planets — machine learning — deep neural networks

1 INTRODUCTION

The majority of exoplanets discovered to date reside in systems which comprise of three or more components (see NEA; Akeson et al. 2013). In such a regime, the analytic solution of the two body problem is not directly applicable and, in general, the orbits must be computed numerically (Murray & Correia 2010). Further, whilst the two body problem guarantees dynamically stable orbits, three-or-more body systems can become unstable over the span of many orbits, leading to ejections or collisions of one or more members (Murray & Dermott 1999).

When studying a specific three-or-more body exoplanet system, a common task is to regress a model describing the observations in question that, in general, must compute the orbital motion of the system’s components. In many cases, the temporal baseline under analysis is much shorter than the expected timescale for significant departures away from purely Keplerian-like motion, which greatly expedites the analysis (e.g. see Kipping 2011 in the case of exomoons). However, although the observed baseline is short, the system is presumably old and thus must have survived a much greater number of orbits without becoming dynamically unstable. This latter point means that, in principle, regressions

of three-or-more body systems should check the resulting dynamical stability of each trial set of parameters. Due to the high computational cost of numerical stability simulations, this is rarely plausible given modern computational facilities, particularly when performing Bayesian regressions which typically explore millions of possible states.

Conventionally, the approach to this problem is to simply ignore it, test the stability of a small subset of fair samples (Lissauer et al. 2011), or use an approximate analytic metric to test stability, such as the Hill criterion (Deck et al. 2013). Recently, there has been interest in adapting the latter approach from using approximate analytic formulae to test stability at each trial, to calling a pre-trained machine learning algorithm capable of rapidly assessing stability. Specifically, Tamayo et al. (2016) demonstrated the plausibility of this approach in application to compact multi-planet systems. In this work, we consider another important case study to be that of circumbinary planets.

Long-period ($\lesssim 300$ d), giant ($R_p > 6 R_{\oplus}$) circumbinary planets appear to be as common as those orbiting single stars (Armstrong et al. 2014). No short period circumbinary planets are presently known¹, which is expected given the

* E-mail: cl3425@columbia.edu

¹ Kepler-47b is the current shortest period circumbinary planet with $P \simeq 50$ days (Orosz et al. 2012).

unstable nature of such orbits due to perturbations from the binary itself (Holman & Wiegert 1999). Since the highly successful transit method is heavily biased against long-period planets (Kipping & Sandford 2016; Gongjie et al. 2016), this means that only a handful of circumbinary planets are presently known. However, the continual accumulation of photometric data sets on overlapping fields, such as TESS (Ricker et al. 2015), NGTS (Wheatley et al. 2013) and PLATO (Rauer et al. 2014), means that more discoveries can be expected of these remarkable exoplanet systems.

The most common approach to evaluating the stability of circumbinary planets is the analytic formula presented in Holman & Wiegert (1999), who regressed a second-order polynomial to a suite of dynamical simulations. However, as noted in that work, islands of instability existed which were not captured by this simple formalism. Since many circumbinary planets appear to reside close to the Holman & Wiegert (1999) critical orbital radius (Welsh et al. 2014), there is a pointed need to test the long-term stability of trials explored during a Bayesian regression, to enable tighter, more physically-sound parameter inference. Following the approach of Tamayo et al. (2016), we turn to machine learning to improve upon the Holman & Wiegert (1999) stability criterion with the goal of capturing the islands of instability noted by the authors.

In Section 2, we first describe how we generated a large suite of training data using numerical simulations. In Section 3, we describe our learning algorithm using a deep neural network. In Section 4, we explore the performance of our approach, particularly in comparison to the existing method of Holman & Wiegert (1999). Finally, we discuss possible applications of our method and future areas for development in Section 5.

2 TRAINING DATA

2.1 Numerical simulations with REBOUND

In order to obtain the training data for our deep network, we decided to use the REBOUND N-body integrator first developed by Rein & Liu (2012). Since first publication, REBOUND has evolved to include IAS15, a non-symplectic integrator with adaptive time-stepping (Rein & Spiegel 2015). We use IAS15 as our integrator of choice. Within the REBOUND environment, we set up a circumbinary planet system with two stars orbiting each other with a semi-major axis of a_{bin} and orbital eccentricity e_{bin} . The planet is chosen to orbit the binary on an initially circular, coplanar orbit with semi-major axis a_p . We ran 10^6 REBOUND experiments each comprising of ten simulations, with each simulation lasting ten thousand binary periods. Experiments were aborted if the planet met our ejection criterion described later in Section 2.2.

For each simulation, we uniformly sampled the mass ratio, μ , from values between 0 and 0.5, where

$$\mu \equiv \frac{m_a}{m_a + m_b}, \quad (1)$$

where $m_a \leq m_b$, and the binary eccentricity, e_{bin} , from values between 0 and 0.99. We then sampled the initial semi-major axis of the planet uniformly from an envelope of $\pm 33\%$ surrounding the empirically derived Holman &

Wiegert (1999) stability criterion for a circumbinary planet², which is given by

$$\begin{aligned} a_{\text{HW99}} = & (1.60 \pm 0.04) + (5.10 \pm 0.05)e \\ & + (-2.22 \pm 0.11)e^2 + (4.12 \pm 0.09)\mu \\ & + (-4.27 \pm 0.17)e\mu + (-5.09 \pm 0.11)\mu^2 \\ & + (4.61 \pm 0.36)e^2\mu^2. \end{aligned} \quad (2)$$

Here, a_{HW99} is the critical semi-major axis given in units of binary separation, since gravity’s lack of scale allows us to use dimensionless units. Orbital elements are Jacobi elements, so positions, velocities, and other orbital elements are centered about the binary center of mass.

To take phase into account, for every sample, ten initial binary phases were drawn uniformly from $[0, 2\pi)$, while keeping the planet phase at zero. If any one of these ten simulations led to an unstable orbit, the grid point was labelled as “unstable”; otherwise, it was “stable”. In total, this meant that ten million unique REBOUND simulations were executed. The stability label of each of the 10^6 grid points was saved and used for training our machine learning algorithm later.

2.2 Stability criterion

Systems can become unstable by the planet being either ejected from the system, or colliding with one of the stars. The former instance can be tested by evaluating whether the radial component of the planet’s velocity, v_r , exceeds the escape velocity of the binary pair, v_{esc} , indicating that the planet will escape to infinity. Rather than formally test for collisions, which requires setting physical radii, we label cases where the planet’s orbit passes interior to that of the binary orbit as being “unstable”.

In Figures 1 & 2, we show two typical examples of a random system which was labelled as “stable” and “unstable”.

2.3 Islands of instability

As can be seen later in Figure 3, the loci of stable points in $\{e_{\text{bin}}, a_p/a_{\text{bin}}\}$ parameter space is described not just by a broad curve, which represents the Holman & Wiegert (1999) critical radius, but also numerous “islands of instability”, to quote the original authors. A machine learning algorithm capable of capturing these islands would lead to a significant improvement in the accuracy of predicting long-term stability versus the simple polynomial form of Holman & Wiegert (1999). These islands are driven by mean motion resonances, and occur at regular intervals in period ratios going as 2:1, 3:1, 4:1, etc.

Due to these resonances, naively using the Holman & Wiegert (1999) stability criterion sometimes misclassifies stability up to a certain distance from a_{HW99} . We conducted a quick check for the minimum-sized envelope containing all such misclassifications, finding that it was sufficient to automatically classify areas further than 120% of the a_{HW99} as

² We initially experimented with 10% to 50% envelopes, but found the 33% envelope was sufficient to encompass the islands of instability, yet compact enough to focus on the areas of interest.

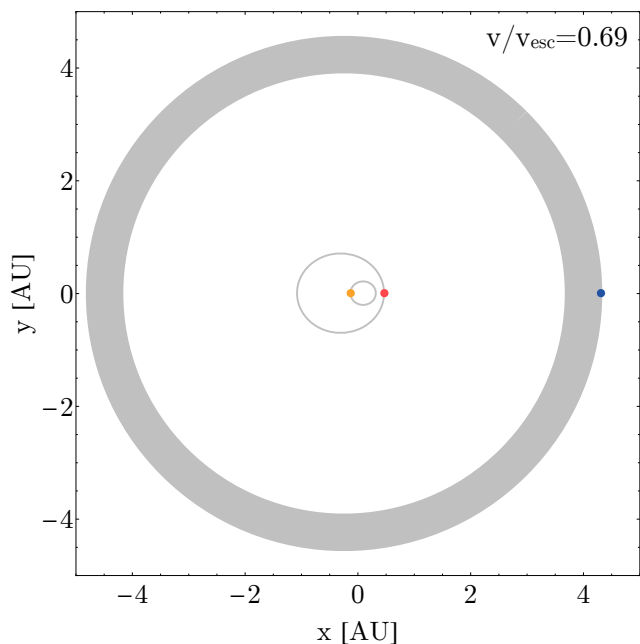


Figure 1. Example of a stable system after ten thousand binary periods. Initial parameters were e_{bin} of 0.4, μ of 0.5, and a_p of 20% greater than the Holman & Wiegert (1999) criterion for the given $\{e_{\text{bin}}, \mu\}$.

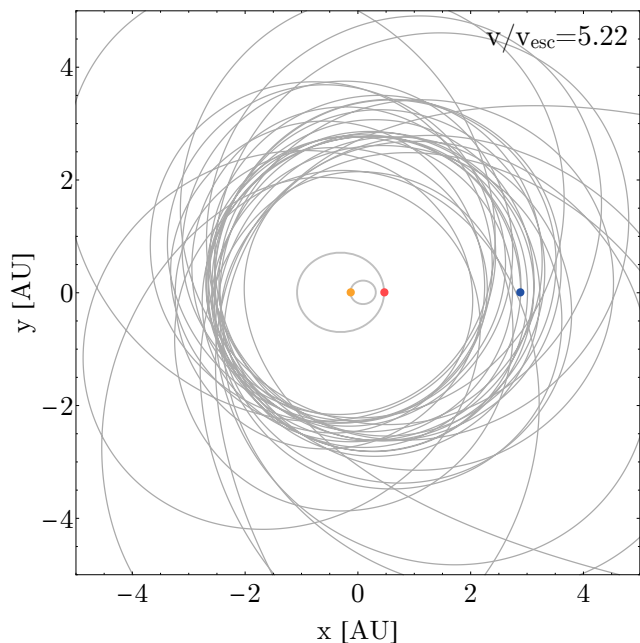


Figure 2. Example of an unstable system after a few dozen binary periods. Initial parameters are e_{bin} of 0.4, μ of 0.5, and a_p of 20% smaller than the Holman & Wiegert (1999) criterion for the given $\{e_{\text{bin}}, \mu\}$.

stable and those interior to 80% of a_{HW99} as unstable. The network was therefore trained on the 600826 samples that fell within the 20% envelope.

To accomodate calls to our algorithm which exceed the 20% region, we simply use an if-statement to assign “stable” if above and “unstable” if below.

3 SUPERVISED LEARNING

3.1 Deep Neural Networks (DNNs)

Whilst Tamayo et al. (2016) predicted the orbital stability of planets in compact multi-planet systems using the XG-Boost v0.6 algorithm (Chen & Guestrin 2016), we elected instead to employ deep neural networks (DNNs), which are comprised of layers through which data is propagated in order to make classifications and predictions. DNNs have been demonstrated to be powerful tools in predictive applications, including already within the field of exoplanetary science (for example see Kipping & Lam 2017, which also includes a brief pedagogical explanation of neural networks).

In this work, we used the `keras` neural network `Python` library rather than construct our own implementation, largely because the DNN required was deeper and more intricate than that used in our earlier work of Kipping & Lam (2017).

3.2 Network architecture

DNNs make predictions by taking a set of N -dimensional inputs and passing the data through “hidden” layers of neurons, in which nonlinear activation functions transform the data. Hidden layers are linked by synapse-like weights that transform the data linearly. The output of the network - here, a binary classification of stable or unstable - is compared with the true results, and the error calculated by some loss function. Our learning algorithm employs back-propagation, which is the chain rule applied to the loss function with respect to the parameter weights. In this manner, the learning algorithm optimizes the loss function by gradient descent. This DNN implementation is typically referred to as a multi-layer perceptron (MLP).

Several key decisions factored into the neural net’s architecture. These include the number of hidden layers, the number of neurons in these hidden layers, the activation functions, the loss function, and dropout.

We used a fairly standard design, comprised of six layers of 48 hidden neurons each, using `relu` (rectifier linear unit) and sigmoid activation functions, `keras`’s `binary_crossentropy` loss function, and the `rmsprop` optimizer. The `relu` activation function, which lives in the hidden layers, is defined as

$$f(x) \equiv \max(0, x). \quad (3)$$

The sigmoid activation function, which lives in the single-neuron output layer, outputs a probability from which classes can be produced and is defined as

$$f(x) = \frac{1}{1 + e^{-x}}. \quad (4)$$

The **rmsprop** optimizer normalizes a moving average of the root mean squared gradients (described in detail within the package documentation at [this URL](#)).

Dropout is a technique to avoid overfitting, an issue endemic to models as complex as DNNs. By setting the dropout rate of a hidden layer, one can adjust the probability at which any hidden neuron and its associated weights drop out of the training set for any particular pass through the neural net. Over many passes, different thinned versions of the DNN are trained on the data, resulting in neurons that depend less on each other for learning, which is also known as a decrease in “co-adapting”. Compared to the classic L2 and L1 regularization methods, dropout has been shown to guard against overfitting better for neural networks (Srivastava et al. 2014).

3.3 Feature selection

Since we sought to compare our model against the previous literature, namely the Holman & Wiegert (1999) criterion, we initially only trained our DNN on the same three variables of that work: e_{bin} , μ and (a_p/a_{bin}) . However, we found that even after experimenting with the network architecture, training sets and learning algorithms, the DNN was unable to reliably recover the islands of instability.

The inability of our initial DNNs to capture the islands motivated us to add an additional fourth training feature. Specifically, since the islands are located at mean motion resonances, we decided to add a new feature describing how far away from one of these resonances a trial semi-major axis is. We refer to this term as the “resonance proxy”, ε , in what follows and define it mathematically as

$$\varepsilon \equiv \frac{\zeta - \lfloor \zeta \rfloor}{2}, \quad (5)$$

where $\lfloor \zeta \rfloor$ is the floor of the ratio of semi-major axes converted to orbital period space via Newton’s version of Kepler’s Third Law, such that

$$\zeta(a_p, a_{\text{bin}}) = (a_p/a_{\text{bin}})^{3/2} \quad (6)$$

After introducing this fourth feature, we found dramatically improved performance of the DNN in terms of capturing the islands of instability, and thus adopted the feature in what follows.

3.4 Iterative learning

When training a DNN, one generally aims to pass the training data through the network iteratively until the weights of the neural net are satisfactorily tuned. To achieve this, we increased the number of training rounds, measured in “epochs”, until the loss on the validation set stopped significantly decreasing. An “epoch” is simply a forward pass through the network and the subsequent back-propagation for all training examples. The number of epochs, then, is the amount of training done before validating the model.

We trained the DNN over several different choices for the maximum number of epochs, ranging from 10 to 250. In general, we found that even after 10 rounds the weights

were well-tuned, which we assessed by comparing the cross-validation precision-recall curves resulting from each and described later in Section 4.3. The learning was relatively fast, taking under 12 seconds per epoch on a MacBook Air. In our final implementation, we elected to use the 100 epoch trained network, whose performance is described quantitatively in Section 4.

4 NETWORK PERFORMANCE

4.1 Capturing the islands of instability

We find that our DNN, as desired, is able to accurately reproduce the islands of instability first noticed by Holman & Wiegert (1999), but not captured by their second-order polynomial function. This can be seen in Figure 3 where we show a slice through parameter space for a fixed μ set to 0.1. Here, we generate 10^5 random new samples in $\{e_{\text{bin}}, (a_p/a_{\text{bin}})\}$ parameter space within the $\pm 33\%$ envelope used earlier but hold μ constant at 0.1 each time, thereby generating a new validation set across a 2D slice. This presentation enables us to easily visualize the islands of instability (left panel) yet also see that in our re-parameterized domain, we are able to accurately predict these islands using our DNN (right panel).

4.2 Execution time

With the learning finished and weights pre-set in the network, any DNN is generally expected to be very fast in making forward predictions. Indeed, on a MacBook Air, the call time for making predictions on 10^5 validation examples is approximately 29 seconds, or about 3 ten-thousandths of a second per validation example. Such a computation time is on the same order of magnitude as typical forward models for describing exoplanet transit observations - for example, the popular transit package **batman** requires around 0.4 milliseconds per call with non-linear limb darkening³ (Kreidberg 2015).

Accordingly, our DNN is fast enough to be practical for on-the-fly Bayesian samplers that potentially need to call the routine many millions of times. Such an approach allows for the computing of a posterior probability that accounts for dynamical stability, where the simplest implementation truncates unstable samples to a zero density.

4.3 Accuracy, Precision, and Recall

When computing statistics by which to evaluate our model, it was important that we not simply apply our DNN directly on the trained data but rather apply it to a previously unseen set, known as a validation set. Accordingly, we generated a new random batch of 10^5 REBOUND simulations within the same bounding region as that originally trained on. We then applied our DNN and tallied the true positive (TP), false positive (FP), true negative (TN), and false negative (FN) rates to generate the accuracy, precision, and recall plots shown in Figure 4. As evident from the figure, our DNN

³ Although **batman** does not natively handle circumbinary planets, which would likely increase this computation time.

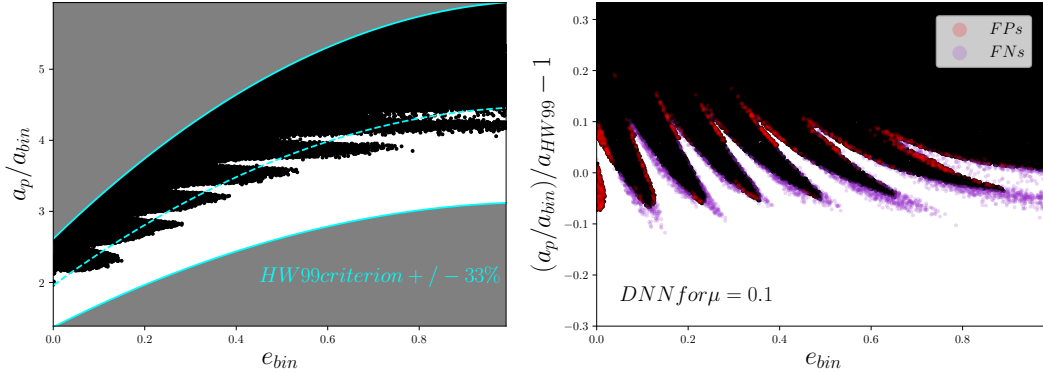


Figure 3. *Left panel:* 10^5 randomly generated, initially circular, coplanar circumbinary planets, where the binary’s eccentricity is varied (x -axis) and the planet’s relative semi-major axis is varied (y -axis). Islands of dynamical instability, as first noted by Holman & Wiegert (1999) [HW99], appear at mean motion resonances yet are not captured by the HW99 polynomial (blue dashed). *Right panel:* Stability predictions from our neural net for the same 10^5 points versus REBOUND simulations. The net was trained on different data, yet is able to capture the islands of instability with a low rate of false-positives (FPs) and false-negatives (FNs). To better visualize the islands of instability, we re-parameterize, treating the Holman-Wiegert criterion as a baseline by dividing the semi-major axis ratio by the criterion and subtracting by one.

indeed out-performs the Holman & Wiegert (1999) criterion, which supports our earlier comparison in Figure 3. This is to be expected given that our DNN has a far larger number of weights than the coefficients describing the Holman & Wiegert (1999) polynomial, allowing it to better express phenomena as complex as the islands of instability.

We compared our DNN with the Holman & Wiegert (1999) criterion using three statistics based on TP, FP, TN, and FN. One basic and useful way to quantify the performance of a binary classifier is accuracy, which is the number of correct classifications as a fraction of total cases. It is defined as

$$\text{accuracy} \equiv \frac{\text{TP} + \text{TN}}{\text{TP} + \text{TN} + \text{FP} + \text{FN}}. \quad (7)$$

Taking the entire suite of validation samples, we find that the accuracy of the Holman & Wiegert (1999) criterion is 93.7%, whereas the DNN achieves 97.1% accuracy over the same region. However, the outer edges of this region are deep into stable and unstable territories, where both approaches have a relatively easy job of picking out the correct answers. To more rigorously evaluate the models, we filter our validation set down to a sub-sample closely surrounding the Holman & Wiegert (1999) boundary. We vary the envelope sequentially in small steps, starting from a very tight envelope and gradually expanding out to the far regions, and in each case compute the accuracy of the two approaches.

The results are shown in the left panel of Figure 4, where one can see that the DNN out-performs the Holman & Wiegert (1999) criterion across the entire range of parameter space considered. As expected, one can see the two functions converge as the envelope grows towards infinity, where the border-line cases become an increasingly negligible fraction of the overall sample. We find that the Holman & Wiegert (1999) criterion approaches a pure random Bernoulli process for very tight envelopes, which is generally to be expected. In contrast, the DNN performs well even at the boundary

and reaches its lowest accuracy of 86.5% close to the boundary. These results allow us to predict that our DNN will be able to deliver $\geq 86.5\%$ accuracy for predicting the stability of circumbinary planets on initially circular, coplanar orbits.

Two other statistics that are common in classifier evaluation are precision, which is defined as the fraction of positive predictions that are actually true, and recall, which is the fraction of true examples that were predicted to be positive. Mathematically, they can be defined as follows:

$$\text{precision} \equiv \frac{\text{TP}}{\text{TP} + \text{FP}} \quad (8)$$

$$\text{recall} \equiv \frac{\text{TP}}{\text{TP} + \text{FN}} \quad (9)$$

Tamayo et al. (2016) evaluated the performance of their network using the classic precision-recall framework, which is typically well-suited for comparing classifiers whose output probabilities can be thresholded. Whereas the thresholds of the Lissauer-family models they evaluated against are varying Hill-sphere separations, the Holman & Wiegert (1999) criterion only predicts stability based on a single threshold: whether or not a planet’s semi-major axis is above or below the curve of the polynomial. Instead of plotting precision against recall, we consequently plotted each against incrementally smaller envelope sizes, as we did with accuracy. While our DNN marginally outperforms the Holman & Wiegert (1999) criterion for the full envelope, with 97.5% versus 96.5% precision and 96.8% versus 91.4% recall, it demonstrates a slower drop in precision and recall as the envelope shrinks. In the smaller-envelope regions of the islands of instability, the performance difference widens to greater than 20% for precision and 35% for recall.

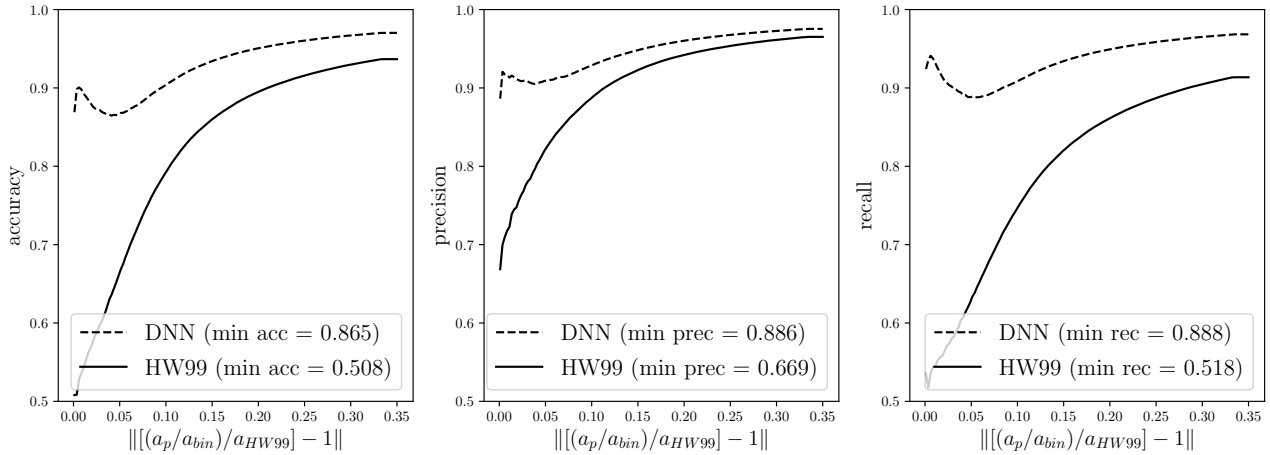


Figure 4. *Left panel:* accuracy *Middle panel:* precision *Right panel:* recall

ing the full envelope as the set of all samples where the absolute value of the planet’s semi-major axis is less than 33%, we observe that our DNN only marginally outperforms Holman-Wiebert on accuracy, precision, and recall. We express the envelopes by re-parameterizing the semi-major axis ratio of planet to binary, dividing it by the polynomial from [Holman & Wiegert \(1999\)](#) to normalize, and subtracting by one to center the islands of instability at zero. Moving left along the x-axis, we shrink the envelope, increasing the dominance of the islands - which are the most difficult to capture - in the validation set. Overall, while Holman-Wiebert converges towards a random Bernoulli process, our DNN persists near 90% for accuracy, precision, and recall.

5 DISCUSSION

In this work, we have demonstrated that a deep neural network (DNN) is able to predict the dynamical stability of circumbinary planets on initially coplanar, circular orbits with greater accuracy, precision, and recall than the previous state-of-the-art: a polynomial function presented in [Holman & Wiegert \(1999\)](#). Our paper builds upon the recent work of [Tamayo et al. \(2016\)](#), who showed that machine learning techniques are well-suited for predicting the stability of multi-planet systems (indeed that was our original applied system too when starting this work). It also provides another powerful demonstration that machine learning is well-suited for binary classification problems in exoplanetary science, such as our previous work using DNNs to predict whether a known planetary system has an additional outer transiting planet ([Kipping & Lam 2017](#)).

By measuring the accuracy, precision, and recall of our DNN predictions on validation sets, we find that our DNN consistently outperforms the [Holman & Wiegert \(1999\)](#) stability criterion, especially in its ability to capture the islands of instability caused by mean motion resonances described in the original paper of [Holman & Wiegert \(1999\)](#). Over the entire region simulated, which spans $\pm 33\%$ of the [Holman & Wiegert \(1999\)](#) criterion, we find that our DNN modestly outperforms the criterion in accuracy, precision, and recall. However, as we decrease the envelope size from $\pm 33\%$ towards 0% so that the islands of instability dominate the validation set, both classifiers face a tougher challenge, with the [Holman & Wiegert \(1999\)](#) criterion approaching a random Bernoulli process and our DNN hovering slightly below 90% accuracy and precision, and slightly above 90% recall. Although our simulations are averaged over random initial phases, it may be that improving metrics such as accuracy beyond this point will be fundamentally limited by the chaotic nature of quasi-stable orbits on the boundary. Despite experimentation with our network configuration, we

were unable to make any improvements to the performance beyond the version described in this work.

We would like to highlight that our work by no means devalues the polynomial-based approach of [Holman & Wiegert \(1999\)](#). Indeed, our training was greatly aided by this previous seminal work, which allowed us to immediately focus in on the region of interest. Further, such analytic formulae provide opportunities for re-parameterization (although we did not pursue this directly on our trained data set), which could also benefit machine learning algorithms.

Our work has assumed a circular, coplanar initial orbit for the planet, as well as test mass particles. For any plausible parameters, the stability boundary extends at least a few tens of stellar radii, so the effects of tides and GR can be ignored, since they are negligible compared to the libration timescale inside the mean motion resonances. Exploring eccentric, initially non-coplanar orbits would seem to be of particular importance for future work, since several known circumbinary planets indeed have small eccentricities. Another possible relevant addition to the feature set is the initial binary phase, which we had accounted for by sampling uniformly as described in Section 2.1. We hope that our work, particularly the realization of using resonance-proxy as an extra feature, may aid and guide those attempting to build more sophisticated classifiers in the future.

The main motivation and obvious application for this work is to apply the classifier during the act of Bayesian regression of circumbinary planet systems. Often these algorithms attempt millions or even billions of trial solutions, which may appear reasonable solutions in terms of likelihood yet dive into regions of parameter space where stability is questionable. In such cases, our classifier could be practically used on-the-fly to evaluate the stability of each trial, and thus assign a stability probability which could be multiplied by the likelihood. The simplest way to do this would

be to use the binary classification output directly (i.e. the probability is either zero or unity).

We finish by highlighting that machine learning techniques are well-suited for problems such as dynamics, where we have in hand the ability to generate essentially arbitrarily large training sets. Deep networks in particular require very large training sets but are able to map non-linear, pathological functions which occur in dynamical problems.

ACKNOWLEDGMENTS

This work has been supported by the Columbia University Center for Career Education’s Work Exemption Program and made use of Columbia’s Habanero shared research computing facility. Simulations in this paper made use of the **REBOUND** code which can be downloaded freely at [this URL](#). This research has made use of the NASA Exoplanet Archive, which is operated by the California Institute of Technology, under contract with the National Aeronautics and Space Administration under the Exoplanet Exploration Program. We thank Daniel Tamayo, Hanno Rein, Gongjie Li, and the Cool Worlds Lab team for helpful comments and conversations in preparing this manuscript.

REFERENCES

- Akeson, R. L., Chen, X., Ciardi, D., et al. 2013, *PASP*, 125, 989
- Armstrong, D. J., Osborn, H. P., Brown, D. J. A., Faedi, F., Gómez Maqueo Chew, Y., Martin, D. V., Pollacco, D. & Udry, S. 2014, *MNRAS*, 444, 1873
- Chen, T. & Guestrin, C. 2016, “Xgboost: A scalable tree boosting system”, arXiv e-print:1603.02754
- Deck, K. M., Payne, M., Holman, M. J. 2013, *ApJ*, 774, 129
- Gongjie, L., Holman, M. J. & Tao, M. 2016, *ApJ*, 831, 96
- Holman, M. J. & Wiegert, P. A. 1999, *AJ*, 117, 621
- Kipping, D. M. 2011, *MNRAS*, 416, 689
- Kipping, D. M. & Lam, C. 2017, *MNRAS*, 465, 3495
- Kipping, D. M. & Sandford, E. 2016, *MNRAS*, 463, 1323
- Kreidberg, L. 2015, *PASP*, 127, 1161
- Lissauer, J. J., Fabrycky, D. C., Ford, E. B., et al. 2011, *Nature*, 470, 53
- Murray, C. D. & Dermott, S. F. 1999, *Solar System Dynamics*. Cambridge Univ. Press, Cambridge
- Murray, C. D. & Correia, A. C. M. 2010, in *Exoplanets*, ed. S. Seager (Tucson, AZ: Univ. of Arizona Press), 15
- Orosz, J. A., Welsh, W. F., Carter, J. A., et al. 2012, *Science*, 337, 1511
- Rauer, H., Catala, C., Aerts, C., et al. 2014, *ExA*, 38, 249
- Rein, H. & Liu, S. F. 2012, *A&A*, 537, A128
- Rein, H. & Spiegel, D. S. 2015, *MNRAS*, 446, 1424
- Rein, H. & Tamayo, D. 2015, *MNRAS*, 452, 376
- Ricker, G. R., Winn, J. N., Vanderspek, R., et al. 2015, *JATIS*, 1, 014003
- Srivastava, N., Hinton, G., Krizhevsky, A., Sutskever, I. & Salakhutdinov, R. 2014, *Journal of Machine Learning Research*, 15, 1929.
- Tamayo, D., Silburt, A., Valencia, D., et al. 2016, *ApJ*, 832, 22
- Welsh W. F., Orosz, J. A., Carter, J. A., Fabrycky, D. C. 2014, *Proc. IAU Symp.* 293, *Formation, Detection, and Characterization of Extrasolar Habitable Planets*. Kluwer, Dordrecht, 125
- Wheatley, P. J., Pollacco, D. L., Queloz, D., et al. 2013, *EPJ Web Conf.*, 47, 13002
- Wisdom, J. & Holman, M. J. 1999, *AJ*, 102, 1528

This paper has been typeset from a $\text{\TeX}/\text{\LaTeX}$ file prepared by the author.